IOP Conf. Series: Materials Science and Engineering **145** (2016) 032012 doi:10.1088/1757-899X/145/3/032012

Setting up the drying regimes based on the theory of moisture migration during drying

M Vasić[1] and Z Radojević [1]
[1] "Institute for testing of materials", Bulevar vojvode Mišića 43 1100 Belgrade, Serbia

E-mail: milos.vasic@institutims.rs

Abstract. Drying is energy intensive process which has important effect on the quality of the clay tiles that are dried commercially. Chamber and tunnel dryers are constantly improving. Better technical equipment and operational strategies have lead to higher quality of the dried clay products. The moisture migration during isothermal drying process can be visually traced on the curve that represents the relationship between variable effective moisture diffusivity (MR) with time (t). Proposed non isothermal drying regimes were consisted from several isothermal segments. For the first time, the choice of isothermal segments specification and its duration was not specified by experience or by trial-and-error method. It was detected from the isothermal curves Deff – MR in accordance with the theory of moisture migration during drying. Proposed drying regimes were tested. Clay roofing tiles were dried without cracks. Dried clay roofing tiles has satisfied all requirements defined in EN 1304 norm related to the shape regularity and mechanical properties.

1. Introduction

Drying is a complex process involving simultaneous heat and mass transfer between the body and the surrounding atmosphere. The whole process consists of several periods characterized with different mechanisms of drying. The theory of moisture migration and modeling of drying process has been the subject of many studies [1 - 4]. The plot of effective moisture diffusivity vs. moisture content (Deff - MR curve) is a good indicator to evaluate and present an overall mass transport property of moisture during isothermal drying. There are many papers relating to determination of the Deff – MR curve [5-7]. The facts that capillary flow is predominant mechanism within the constant drying period, while in the falling drying period, the evaporation – condensation and vapor diffusion are the predominant mechanisms, has wan general recognition for the explanation of moisture transfer in porous media. The method useful to trace and quantify all possible mechanisms of moisture transport and their transitions during the isothermal drying process was recently reported [8].

This study has several objectives. The first one was to calculate the variable effective diffusivity, to divide drying curve in segments and to identify all possible mechanisms of moisture transport within a clay roofing tile for several different experiments, in which draying air parameters were constant, using the previously mentioned method [8]. The second and main objective of this study was to analyze all obtained isothermal data to create a link with the comprehensive theory of moisture migration during drying and to set up the non isothermal drying process.

2. Materials and Methods

Experiments were carried out with the raw material obtained from the largest roofing tile manufacturer in Serbia. Initial characterization of the raw material which has included: determination of particle size distribution (PSD), standard silicate chemical analysis (SSA), qualitative and semi-quantitative XRD and TGA/TG analysis was reported in studies [9, 10]. After initial characterization, the raw material was homogenized and prepared for the forming process. It was first dried at 60^{o}C and then milled down in a laboratory perforated rolls mill. Subsequently, the raw material was moisturized and milled in a laboratory differential mill, first with a gap of 3 mm and then of 1 mm**.**

Laboratory roofing tile samples 120 × 50 × 14 mm were formed, from the previously prepared clay, in a laboratory extruder "Hendle" type 4, under a vacuum of 0.8 bar. Formed sample were packed into plastic bags which were afterwards sealed and put into a glass container with lid. Glass containers with samples were kept in the air-conditioned room in which temperature and relative humidity were maintained respectively at 25^{0}C and 65%. This procedure allows the minimal moisture content fluctuations within the stored samples.

Series of isothermal drying curves was reordered. Laboratory recirculation dryer in which drying parameters (humidity, temperature, and velocity) could be programmed, controlled and monitored was used. Regulation of wet air parameters within the range of 0-125 °C, 20-100 % and 0-3.5 m/s with accuracies of ±0.2 °C, ±0.2 % and ±0.1 % for temperature, humidity and velocity, respectively, was limited by the laboratory dryer design. The mass of the samples and their linear shrinkage were continually monitored and recorded during the experiments. The accuracies of these measurements were 0.01 g and 0.2 mm, respectively. Experimental conditions presented at table 1 were used in the present study. Each experiment was repeated 2 times.

Table 1. Experimental conditions - isothermal drying regimes.

Experiment	Group	Air humidity, V / %	Air temperature, T / °C
1	I	80	30
2	I	80	40
3	II	70	40
4	II	70	45
5	III	60	40
6	III	60	45

The methodology and program "Deff Calculator" presented in the [8] was used to calculate the functional dependence of the effective diffusivity with moisture content (Deff – MR), to divide obtained curves in segments and to identify all possible mechanisms of moisture transport within the each drying segments. Roofing tiles samples were afterwards dried to constant mass. Dried samples were heated in oxygen atmosphere with the heating rate of 1.4^{0}C/min from room temperature up to 610^{0}C, and further with the heating rate of 2.5^{0}C/min up to the 1000^{0}C. Samples were kept at 1000^{0}C for 2 hours. Flexural strength was determined on dried (DSFS) and fired samples (FSFS) using the standard procedure described in EN 538 norm.

Obtained data were analyzed and used to set up several non isothermal drying regimes. Drying air parameters which were maintained in each proposed drying regimes are presented in table II. Duration of the approximately isothermal drying segments was detected from the isothermal curves Deff – MR. Each experiment was repeated 2 times. Dried tiles were then dried to constant mass and fired using the same heating rate as one previously mentioned. DSFS and FSFS were determined. Twist (TC) as well as longitudinal camber (RL) and transverse camber (RT) coefficient were determined on fired samples using the standard procedure described in EN 1024 norm.

Table 2. Experimental conditions - proposed drying regimes.

Eksperiment	Segment				
	I	II	III	IV	V
7	Ekps. 1	Eksp. 2	Eksp. 3	Eksp. 4	70% / 40^{0}C
8	Eksp. 2	Eksp. 3	Eksp. 5	Eksp. 6	70% / 40^{0}C

3. Results and discussion

All possible mechanisms of moisture transport and their transition from one to another during the constant and the falling drying period for isothermal experiments are well identified and are shown at figure 1. Drying segments along with mechanisms that can take place in them according to the reference [8] are summarized at table 3.

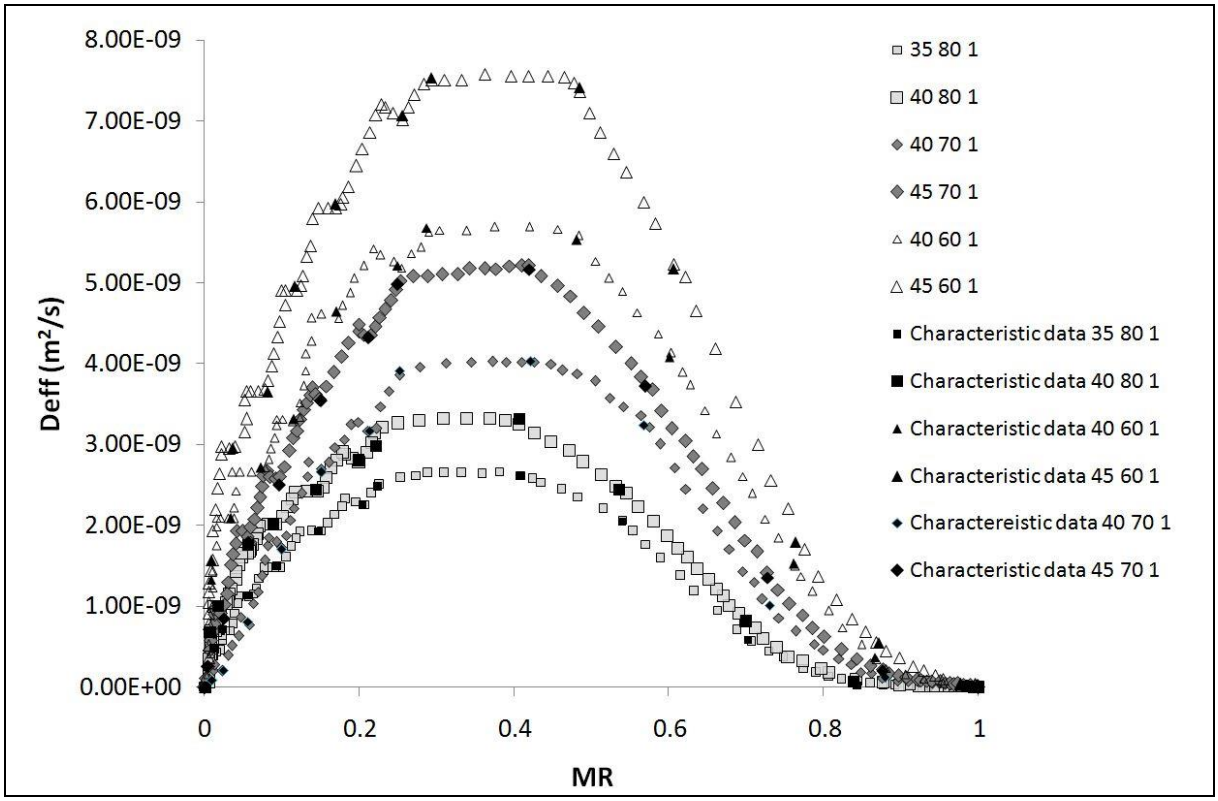

Figure 1. Estimated Deff – MR curves for isothermal experiments.

The procedure for setting up the non isothermal drying regime, that is consistent with the theory of moisture migration during drying (see table 3) was based on the principle of controlling the mass transport during the drying process and has demanded to divide the drying process into 5 segments. In each of these segments approximately isothermal drying conditions were maintained (see table 2).

The main functions of the first segment are to restrain the moisture transport (evaporation), through the boundary layer between material surface and the bulk air, and to heat the ceramic body to the temperature of the drying air. That is the reason why high values of the drying air humidity in the first segment were selected. In order to fulfill previously mentioned requirements, this drying segment is over when characteristic point C is reached. During the second drying segment external (surface evaporation) and internal transport (of liquid water from the ceramic body up to the surface) has to be increased and simultaneously harmonized in such way that the drying surface remain fully covered by a water film. That is the reason why in most cases drying air humidity in this segment is reduced. Its

absolute value is still relatively high. This will increase the evaporation driving force and consequently will speed up the drying process. Drying air temperature in this segment may slightly increase compared to the previous segment. This will moderately increase the capillary transport as well as the drying rate. The second segment starts and ends when characteristic point C and D ("upper critical point") are respectively reached.

Table 3. Possible drying mechanisms according to reference [8].

Drying segment	Transport of liquid water	Transport of vapor	Additional explanation
A B	- Capillary pumping flow through the biggest capillaries	/	0A – initial heating AE - constant period FL - falling period
B C	- Capillary pumping flow through macro capillaries - hydrodynamic flow	/	
C D	- Capillary pumping flow through mezzo capillaries - Hydrodynamic flow	/	D – "upper critical" point "funicular state" (continuous threads of moisture are present in the pores) Surface is completely wet Front start to recede into body
D E	- Capillary pumping flow (from capillaries in funicular state) - Hydrodynamic flow - liquid diffusion in the pores	- hydrodynamic flow	DE – Partially wet surface
E F	- Creeping along the capillary when the liquid is in the funicular state or by the successive evaporation – condensation mechanism between liquid bridges.	- hydrodynamic flow (difference in total pressure)	F - "lower critical" point - "pendular state" (continuous threads of moisture are not presented in the pores) - "last" wet patches disappeared from the surface
F G	the successive evaporation – condensation mechanism between liquid bridges of pendular water	- hydrodynamic flow (difference in total pressure)	
G H	the successive evaporation – condensation mechanism between liquid bridges of pendular water	Stefan Flux (difference in partial pressure) - hydrodynamic flow (difference in total pressure)	
H I	The evaporation – condensation mechanism was still active but is decreasing rapidly	hydrodynamic flow (difference in total pressure)	
I J	/	Molecular diffusion	
J K	/	Transition diffusion	
K L	/	Knudsen diffusion	

The third and fourth segment represents together a transitional drying period in which the sample is gradually shifting from "funicular" to the "pendular" state. The main difference between these two states is that in the “funicular” state, continuous threads of moisture are present in the pores, while in the “pendular” state this is not the case. A partially wet surface is able to provide a constant or a falling drying period depending on the fraction of wet surface and the boundary layer thickness. A higher fraction of wet surface and a thicker boundary layer produces and favors a constant drying rate period, while a smaller fraction of the surface and a thinner boundary layer shell favors and produces a falling drying rate. The main function of the third segment is to provide the conditions that will lead to the fact that partially wet surfaces provide a constant rate of drying. That is the reasons why the humidity and temperature of the drying air within the segment III has to be carefully selected. Further reduction of the drying air humidity (see table 2) will increase the evaporation driving force (external surface evaporation) and consequently will speed up the drying process. Drying air temperature in this segment may slightly increase compared to the previous segment. This will increase the capillary transport as well as the drying rate. The third segment starts and ends when characteristic point D and E are respectively reached.

Within the segment IV, the fraction of the wet surface decreased until the “last” wet patches disappeared from the surface. The moisture content had decreased and the gas bubbles attained the dimensions of the pores, breaking the continuous threads of moisture in the pores. When the liquid (capillary) fluxes are broken and the system had reached the “pendular” state, there is no further contraction of the drying body. The main function of this segment is to simultaneously harmonize the liquid transport originating from the pores which are near or just below the “dry” patches on the surface and are still in the funicular state with the liquid flow originating from the surface “wet” patches. That is the reason why drying air humidity in this segment is not reduced (see table 2).
Further increase of the drying air temperature has a positive influence which has lead to the liquid transport enhancement. The fourth segment starts and ends when characteristic point E and F (“lower critical point”) are respectively reached. After segment IV is over (point F is reached), the possibility of the drying body cracking is extremely small. This fact was used to define that the main function of the fifth segment is to maximally facilitate the internal moisture transport up to the surface. That is the reason why drying air humidity in the fifth segment is further reduced while drying air temperature is maximally increased. Characteristic data up to the point F presented on figure 1 are summarized in table 4.

Table 4. Characteristic data for isothermal experiments from point A up to point F.

Exp. / Group		1 I	2 I	3 II	4 II	5 III	6 III
A	t (min)	61	48	46	33	20	18
	MR	0.982	0.985	0.995	0.991	0.976	0.976
B	t (min)	165	152	113	93	53	49
	MR	0.842	0.836	0.879	0.875	0.865	0.870
C	t (min)	284	257	194	174	86	79
	MR	0.702	0.700	0.730	0.727	0.761	0.763
D	t (min)	421	384	281	265	142	130
	MR	0.538	0.535	0.571	0.568	0.600	0.606
E	t (min)	530	488	364	342	191	174
	MR	0.407	0.406	0.422	0.419	0.481	0.484
F	t (min)	774	705	523	496	296	273
	MR	0.223	0.221	0.252	0.248	0.286	0.292
TDT* (min)		1398	1180	1104	1044	700	600

*Total drying time

For the first time, the choice of isothermal segments specification was achieved in accordance with the theory of moisture migration during drying and with the nature and the properties of the clay raw

materials. Duration of the approximately isothermal drying segments was not specified by experience or by trial-and-error method. It was detected from the appropriate isothermal Deff – MR curves (see figure 1 and table 3). General procedure will be explained on the experiment 7. Duration of the first segment was the same as the duration of the drying process in the case of experiment 1 from the beginning up to the characteristic point C. Duration of the second segment was the same as the duration of the drying process in the case of experiment 2 from the characteristic point C up to the characteristic point D. Duration of the third segment was the same as the duration of the drying process in the case of experiment 3 from the characteristic point D up to the characteristic point E. Duration of the fourth segment was the same as the duration of the drying process in the case of experiment 4 from the characteristic point E up to the characteristic point F. Duration of the fifth segment was limited to 90 minutes. This procedure was used to specify the duration of drying segments in each proposed drying regime. Calculated results are presented in table 5.

Table 5. Duration of each drying segment – proposed drying regimes

Drying segment	Segment duration t (min)	
	Eksp. 7	Eksp. 8
1	284	257
2	127	87
3	83	49
4	154	99
5	90	90
TDT	738	582

It is important to define the minimum requirements for dried clay roofing tile which if satisfactory will ensure that the product is able to perform its function. In other words dried clay roofing tiles has to be dried without cracks. Minimal flexural strength of dried and fired samples has to be respectively at least 0.73 and 1.2kN (see EN 1304 norm). The mean value of the twist coefficient (TC) as well as the mean value of the longitudinal (RL) and transverse (RT) cambers calculated as described in EN 1024 norm shall comply respectively with the requirements stated in tables 1 - 3 presented within the EN 1304 norm.

Proposed drying regimes were tested. Clay roofing tiles were dried without cracks. Flexural strength of dried and fired clay tiles (DSFS and FSFS) are presented in table 6.

Table 6. Mechanical properties of dried and fired samples

Experiment	Group	DSFS (kN)	FSFS (kN)
			1000^0C
1	I	0.99	2.73
2	I	0.97	2.65
3	II	0.92	2.67
4	II	0.82	2.65
5	III	0.80	2.12
6	III	0.75	2.08
7	non isothermal	0.93	2.65
8	non isothermal	0.81	2.42

The mean TC value as well as the mean RL and RT values for isothermal and non isothermal drying regimes is presented in table 7. Detailed analyze of data presented in table 6 has revealed that: mean TC, RL and RT values within all isothermal experimental groups (I – III), is increasing with the increase of the drying air temperature as well as that under the same drying air temperature, TC, RL and RT values, presented in different experimental groups, is also increasing with the decrease of air relative humidity (see tables 1 and 5).

Table 7. Regularity of shape - twist and cambers coefficients

Experiment	Twist coefficient C (%)	Cambers R (%)	
		Longitudal	Transverse
1	0.29	0.33	0.35
2	0.45	0.50	0.57
3	0.90	0.68	0.74
4	1.23	0.87	0.94
5	0.72	0.79	0.88
6	1.18	1.05	1.11
7	0.48	0.51	0.57
8	0.71	0.69	0.81
Criteria is defined in EN 1304 (Tables 1 – 3)	Allowed deviation for C and R		
	≤ 2%	≤ 2%	≤ 2%

TC, RL and RT values can be used as a good indirect indicator of the stress generation. In other words higher TC, RL and RT values are correlated with the higher stress generation. The drying air with higher temperature and lower relative humidity leads to more rapid generation of the stress in the samples during drying which will result with the lower shape regularity (higher TC, RL and RT coefficients) and lower mechanical properties of the dried samples.

The shortest drying time (TDT) for isothermal and non isothermal drying regimes was respectively registered in experiment 8 and 5 (see tables 2 and 4). The difference between TDT values related to previously mentioned experiments is relatively small. The lowest DSFS and FSFS values along with the highest mean TC, RL and RT values for non isothermal drying regimes was registered in experiment 7. It is important to point out that dried as well as fired clay roofing tiles in each proposed non isothermal experiment have satisfied previously mentioned flexural strength as well as shape regularity (twist and cambers) criteria. That is the reason why in this study the lowest TDT vale was used as a final criterion for selection of the experiment 7 drying regime as optimal (see table 4, experiment 8).

4. Conclusions

The procedure for setting up the non isothermal drying regime that is consistent with the theory of moisture migration during drying has demanded to divide the drying process into 5 segments. For the first time, the choice of isothermal segments specification was achieved in accordance with the theory of moisture migration during drying and with the nature and the properties of the clay raw materials. Duration of the approximately isothermal drying segments was not specified by experience or by trial-and-error method. It was detected from the appropriate isothermal Deff – MR curves. Proposed drying regimes were tested. Dried clay roofing tiles has satisfied all requirements related to the shape regularity and mechanical properties as defined in EN 1304 norm. Finally experiment 8 was chosen as the optimal drying regime.

Acknowledgement

Note: This paper was realized under the project *ИИИ* 45008 which was financed by ministry of education and science of Serbia.

References

[1] Luikov A V 1975 System of differential equations of heat and mass transfer in capillary-porous bodies (review) *Int. Jour. of heat and Mass Transfer* 18(**1)** pp 1-14

[2] Whitaker S 1998 Coupled transport in multiphase systems: A theory of drying *Adv. in Heat Transfer* **31** pp 1-104

[3] Bowen R M 1980 Incompressible porous media models by use of the theory of mixtures *Int. J. of Eng. Science* 18 **9** pp 1129-1148.
[4] Kowalski S J 2000 Toward a thermodynamic of drying process *Chem. Ing. Sciences* **55** pp 1289-1304
[5] Pinto A L and Tobinaga S 2006 Diffusive model with shrinkage in the thin-layer drying of fish muscules *Drying Technology* 24 **4** pp 509-516
[6] Lopez R I I, Espinoza R H, Lozada A P and Alvarado G M A 2012 Analytical model for moisture diffusivity estimation and drying simulation of shrinkable food products *J. Food Eng.* **108** pp 427-435
[7] Chemki S and Zagrouba F 2005 Water diffusion coefficient in clay material from drying data *Desalination* **185** pp 491-498
[8] Vasić M, Grbavčić Ž and Radojević Z 2014 Analysis of Moisture Transfer During the Drying of Clay Tiles with Particular Reference to an Estimation of the Time-Dependent Effective Diffusivity *Drying Technology* 32 **7** pp 829-840
[9] Rekecki R and Ranogajec J 2008 Design of ceramic miscrostructures based on waste materials *Proc. and Appl. of Ceramic* **2** pp 89-95
[10] Rekecki R, Ranogajec J and Kuzmann E 2014 Analiya faznih promena karbonatne gline tokom pečenja metodama mesbauerove spektroskopije i difrakcije X zraka *Izgradnja* 68 **9-10** pp 76-82